

Temperature dependence and non-Condon effects in pump-probe spectroscopy in the condensed phase

Yoshitaka Tanimura and Shaul Mukamel

Department of Chemistry, University of Rochester, Rochester, New York 14627

Received January 27, 1993; revised manuscript received June 10, 1993

We analyze the effects of the coordinate dependence of the transition dipole (non-Condon dipole moment) on impulsive pump-probe spectroscopy at finite temperatures, using expressions for the response functions derived by the path-integral approach. We calculate the difference probe absorption spectrum and show that the non-Condon dipole shifts the absorption to the blue and that the shift increases with temperature.

The multimode Brownian oscillator model^{1,2} provides a convenient means for incorporating nuclear degrees of freedom in optical response functions.³⁻⁹ We recently used a path-integral approach¹⁰ to develop exact closed expressions for the nuclear wave packets in phase space and for the nonlinear response functions for this model.¹¹

In this paper we apply these results to pump-probe spectroscopy. We consider an electronic two-level system, denoted by g (the ground state) and e (the excited state), and frequency ω_{eg} . The optically active vibration of polyatomic molecules in the condensed phase can often be described with a Brownian oscillator model in which the ground state and the excited state are represented by displaced harmonic oscillators. We denote the nuclear mass, the coordinate, the harmonic frequency, and the dimensionless displacement of the oscillators by M , q , ω_0 , and D , respectively. We would like to include relaxation of the optically active mode. This is commonly taken into account by using the Langevin equation. However, the quantum coherence between the heat bath and the vibrational system plays an important role at low temperatures. This effect cannot be taken into account with the classical Langevin equation, and therefore we explicitly introduce a model for a heat bath. The heat-bath system may represent optically inactive vibrational modes, phonons, solvent modes, etc. We assume that the optically active vibration is linearly coupled to a heat bath, with the coordinates, the momentum, the mass, and the frequency of the n th bath oscillator given by x_n , p_n , m_n , and ω_n , respectively. The total Hamiltonian is then expressed as^{11,12}

$$H \equiv |g\rangle H_g(p, q) \langle g| + |e\rangle H_e(p, q) \langle e| + \sum_n \left[\frac{p_n^2}{2m_n} + \frac{m_n \omega_n^2}{2} \left(x_n - \frac{c_n q}{m_n \omega_n^2} \right)^2 \right], \quad (1)$$

where

$$H_g(p, q) \equiv \frac{p^2}{2M} + \frac{1}{2} M \omega_0^2 q^2, \\ H_e(p, q) \equiv \frac{p^2}{2M} + \frac{1}{2} M \omega_0^2 (q + D)^2 + \hbar \omega_{eg}^0. \quad (2)$$

The two states are connected by the optical-dipole interaction

$$H_I \equiv E(t)V \equiv E(t)[|g\rangle\mu(q)\langle e| + |e\rangle\mu(q)\langle g|], \quad (3)$$

where $E(t)$ is the laser field and $\mu(q)$ is the dipole matrix element between the two states that depends on the nuclear coordinate. We assume that the transition dipole has the form

$$\mu(q) = \mu_0 \exp(cq), \quad (4)$$

where c is the coupling constant. Typically in molecular systems c is small ($cq_L \ll 1$, where q_L is the size of the nuclear wave packet), so that $\mu(q) \approx \mu_0(1 + cq)$.

The optical polarization for a third-order optical process is obtained by expanding the density matrix elements in H_I and is expressed as

$$P^{(3)}(t) = i \int_0^\infty dt_3 \int_0^\infty dt_2 \int_0^\infty dt_1 E(t - t_3) E(t - t_2 - t_3) \\ \times E(t - t_1 - t_2 - t_3) \text{tr} \left[V \exp\left(-\frac{i}{\hbar} t_3 H^\times\right) V^\times \right. \\ \left. \times \exp\left(-\frac{i}{\hbar} t_2 H^\times\right) V^\times \exp\left(-\frac{i}{\hbar} t_1 H^\times\right) V^\times \rho_g \right]. \quad (5)$$

Here, ρ_g is the ground equilibrium state of the total system, and we use the superoperator notation defined by $A^\times B \equiv AB - BA$, $A^\times B^\times C \equiv A(BC - CB) - (BC - CB)A$, and so forth, where A , B , and C are ordinary operators. Since each V^\times can act either from the left or from the right, and since $P^{(3)}(t)$ contains V^\times factors, Eq. (5) naturally separates into 2^3 terms denoted by Liouville-space paths.² In practice we need to evaluate only half of these terms, since they always come in Hermitian conjugate pairs, and, for the third-order polarization, we need four Liouville-space paths, denoted by $\alpha = 1 - 4$ (see Fig. 1).

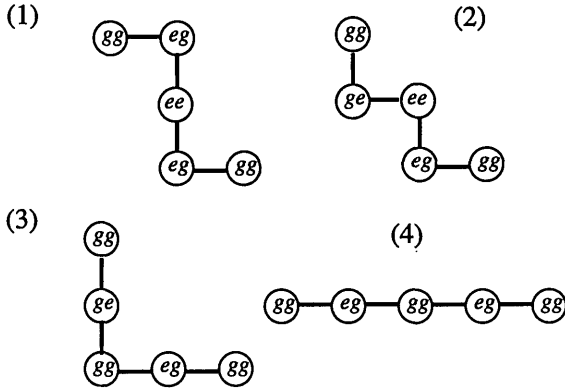


Fig. 1. Liouville-space paths for the third-order response functions. Solid lines denote the dipole interaction V . A horizontal (vertical) line represents an action of V from the left (right) to the density-matrix elements. Starting with gg in the upper left-hand corner, there are eight pathways that lead to the optical coherence eg or ge in the third order. Only half of these pathways [ending in gg , (1)–(4)] are shown. The contributions of the other pathways is the complex conjugate of those shown.

All dynamical characteristics of the system can be expressed in terms of the phase function defined by

$$g_+(t) \equiv \xi^2 \int_0^t dt' \int_0^{t'} dt'' \langle qq(t'') \rangle,$$

$$g_-(t) \equiv \xi^2 \int_0^t dt' \int_0^{t'} dt'' \langle q(t'') q \rangle, \quad (6)$$

where $\langle qq(t) \rangle$ and $\langle q(t)q \rangle$ are the position correlation functions and

$$\xi \equiv MD\omega_0^2/\hbar. \quad (7)$$

To express the results in a compact form, we assign three sign parameters, ϵ_1 , ϵ_2 , and ϵ_3 (see Table 1) to each of the Liouville-space paths. With this notation the optical polarization for a third-order optical process is given by¹¹

$$P^{(3)}(t) = i \int_0^\infty dt_3 \int_0^\infty dt_2 \int_0^\infty dt_1 E(t-t_3)E(t-t_2-t_3)$$

$$\times E(t-t_1-t_2-t_3) \sum_{\epsilon_1, \epsilon_2, \epsilon_3} \mu_0^4 R_{\epsilon_1 \epsilon_2 \epsilon_3}^{(3)}(t_3, t_2, t_1; c)$$

$$+ \text{c.c.} \quad (8)$$

Here the response function is given by

$$R_{\epsilon_1 \epsilon_2 \epsilon_3}^{(3)}(t_3, t_2, t_1; c)$$

$$= \exp[Q_{\epsilon_1 \epsilon_2 \epsilon_3}(t_3, t_2, t_1) + X_{\epsilon_1 \epsilon_2 \epsilon_3}(t_3, t_2, t_1; c)], \quad (9)$$

where

$$Q_{\epsilon_1 \epsilon_2 \epsilon_3}(t_3, t_2, t_1) = -i\omega_{eg}(\epsilon_1 t_1 + \epsilon_3 t_3) - g_{-\epsilon_1}(t_1) - g_{\epsilon_2 \epsilon_3}(t_3)$$

$$- \epsilon_1 \epsilon_3 [g_{\epsilon_1 \epsilon_2}(t_2) - g_{\epsilon_1 \epsilon_2}(t_2 + t_3)$$

$$- g_{-\epsilon_1}(t_1 + t_2) + g_{-\epsilon_1}(t_1 + t_2 + t_3)], \quad (10)$$

with

$$X_{\epsilon_1 \epsilon_2 \epsilon_3}(t_3, t_2, t_1; c)$$

$$= c[\langle \bar{q}_1(\{t\}) \rangle_{\epsilon_1 \epsilon_2 \epsilon_3} + \langle \bar{q}_2(\{t\}) \rangle_{\epsilon_1 \epsilon_2 \epsilon_3} + \langle \bar{q}_3(\{t\}) \rangle_{\epsilon_1 \epsilon_2 \epsilon_3}$$

$$+ \langle \bar{q}_4(\{t\}) \rangle_{\epsilon_1 \epsilon_2 \epsilon_3}] + c^2 \xi^{-2} [\ddot{g}_{-\epsilon_1}(t_1) + \ddot{g}_{-\epsilon_1}(t_1 + t_2)$$

$$+ \ddot{g}_{\epsilon_1 \epsilon_2}(t_2) + \ddot{g}_{-\epsilon_1}(t_1 + t_2 + t_3) + \ddot{g}_{\epsilon_1 \epsilon_2}(t_2 + t_3)$$

$$+ \ddot{g}_{\epsilon_2 \epsilon_3}(t_3) + 2\ddot{g}(0)], \quad (11)$$

$$\omega_{eg} \equiv \omega_{eg}^0 + \lambda, \quad \lambda \equiv MD^2\omega_0^2/(2\hbar), \quad (12)$$

$$\langle \bar{q}_1(\{t\}) \rangle_{\epsilon_1 \epsilon_2 \epsilon_3} = -i\xi^{-1} [\epsilon_1 \dot{g}_{-\epsilon_1}(t_1) - \epsilon_3 \dot{g}_{-\epsilon_1}(t_1 + t_2)$$

$$+ \epsilon_3 \dot{g}_{-\epsilon_1}(t_1 + t_2 + t_3)],$$

$$\langle \bar{q}_2(\{t\}) \rangle_{\epsilon_1 \epsilon_2 \epsilon_3} = -i\xi^{-1} [\epsilon_1 \dot{g}_{-\epsilon_1}(t_1) + \epsilon_3 \dot{g}_{\epsilon_1 \epsilon_2}(t_2 + t_3)$$

$$- \epsilon_3 \dot{g}_{\epsilon_1 \epsilon_2}(t_2)],$$

$$\langle \bar{q}_3(\{t\}) \rangle_{\epsilon_1 \epsilon_2 \epsilon_3} = -i\xi^{-1} [\epsilon_1 \dot{g}_{-\epsilon_1}(t_1 + t_2) - \epsilon_1 \dot{g}_{\epsilon_1 \epsilon_2}(t_2)$$

$$+ \epsilon_3 \dot{g}_{\epsilon_2 \epsilon_3}(t_3)],$$

$$\langle \bar{q}_4(\{t\}) \rangle_{\epsilon_1 \epsilon_2 \epsilon_3} = -i\xi^{-1} [\epsilon_1 \dot{g}_{-\epsilon_1}(t_1 + t_2 + t_3) - \epsilon_1 \dot{g}_{\epsilon_1 \epsilon_2}(t_2 + t_3)$$

$$+ \epsilon_3 \dot{g}_{\epsilon_2 \epsilon_3}(t_3)]. \quad (13)$$

Equation (10) is identical to the phase of the response function with the Condon approximation, which may be derived by use of the cumulant expansion¹; however, the present notation is more convenient for numerical studies.

The probe absorption spectrum, obtained by dispersion of the transmitted probe through a monochromator, is given by¹³

$$S(\omega_2 - \Omega_2) = -2 \text{Im} E_2(\omega_2 - \Omega_2) P^{(3)}(\omega_2 - \Omega_2), \quad (14)$$

where

$$E_2(\omega_2 - \Omega_2) = \frac{1}{(2\pi)^{1/2}} \int_{-\infty}^{\infty} dt \exp[i(\omega_2 - \Omega_2)t] E_2(t), \quad (15)$$

$$P^{(3)}(\omega_2 - \Omega_2) = \frac{1}{(2\pi)^{1/2}} \int_{-\infty}^{\infty} dt \exp[i(\omega_2 - \Omega_2)t] P^{(3)}(t), \quad (16)$$

and Ω_2 is the central frequency of the probe. We assume impulsive pump and probe fields, i.e.,

$$E_1(t) = \theta_1 \delta(t + \tau), \quad E_2(t) = \theta_2 \delta(t), \quad (17)$$

where θ_1 and θ_2 are the pump and the probe areas. For the impulsive pump case, we have

$$S(\omega_2 - \Omega_2; \tau) = S_{ee}(\omega_2 - \Omega_2; \tau) + S_{gg}(\omega_2 - \Omega_2; \tau). \quad (18)$$

Table 1. Auxiliary Parameters for Eqs. (9)–(13)

Liouville Space Path α	ϵ_1	ϵ_2	ϵ_3
1	+	+	+
2	-	+	+
3	-	-	+
4	+	-	+

Here S_{ee} represents the contribution from the Liouville paths $\alpha = 1$ and $\alpha = 2$, which pass through the excited state (ρ_{ee}) during the t_2 time interval, whereas S_{gg} represents the contributions of the other paths $\alpha = 3$ and $\alpha = 4$, which pass through the ground state (ρ_{gg}) during that interval:

$$S_{ee}(\omega_2 - \Omega_2; \tau) = 2 \operatorname{Re} \int_0^\infty dt_3 \exp[i(\omega_2 - \Omega_2)t_3] \\ \times [R_{++}^{(3)}(t_3, \tau, 0) + R_{--}^{(3)}(t_3, \tau, 0)], \quad (19)$$

$$S_{gg}(\omega_2 - \Omega_2; \tau) = 2 \operatorname{Re} \int_0^\infty dt_3 \exp[i(\omega_2 - \Omega_2)t_3] \\ \times [R_{--}^{(3)}(t_3, \tau, 0) + R_{++}^{(3)}(t_3, \tau, 0)], \quad (20)$$

and we set $\mu_0\theta_1 = \mu_0\theta_2 = 1$.

By formulating pump-probe spectroscopy in Liouville space, it becomes possible for us to separate the process into three steps: First the pump beam creates a wave packet during the t_1 period (the doorway state). There are actually two wave packets in the excited-state (hereafter denoted the particle) paths 1 and 2, and the other is the ground state (the hole) coming from paths 3 and 4. These two wave packets then propagate during the delay time between the pump and the probe. This evolution is the most significant information obtained from pump and probe spectroscopy. Finally, the system interacts with the probe, and the signal is generated. We denote the wave packet of the particle and the hole by W_e and W_g , respectively. These wave packets are given by

$$W_{e_2}^{(3)}(p, q; t) = \int_0^\infty dt_1 \int_0^\infty dt_2 E(t - t_2) \\ \times E(t - t_1 - t_2) (4\pi^2 \langle p^2 \rangle_g \langle q^2 \rangle_g)^{-1/2} \\ \times \sum_{\epsilon_1 = \pm} \exp\left\{-\frac{1}{2\langle q^2 \rangle_g} [q - \bar{q}_{\epsilon_1 \epsilon_2}(t_2, t_1; c)]^2\right. \\ \left. - \frac{1}{\langle p^2 \rangle_g} [p - \bar{p}_{\epsilon_1 \epsilon_2}(t_2, t_1; c)]^2\right\} R_{\epsilon_1}^{(1)}(t_1; c) + \text{c.c.}, \quad (21)$$

where

$$\langle q^2 \rangle_g = \xi^2 \ddot{g}_+(0), \quad \langle p^2 \rangle_g = \xi^{-2} M^2 \frac{d^4 g_+(t)}{dt^4} \Big|_{t=0}, \quad (22)$$

$$\bar{q}_{\epsilon_1 \epsilon_2}(t_2, t_1; c) = -i\xi^{-1} [\epsilon_1 \dot{g}_{-\epsilon_1}(t_1 + t_2) - \epsilon_1 \dot{g}_{\epsilon_2 \epsilon_1}(t_2)] \\ + c\xi^{-2} [\ddot{g}_{-\epsilon_1}(t_1 + t_2) + \ddot{g}_{\epsilon_2 \epsilon_1}(t_2)], \quad (23)$$

$$\bar{p}_{\epsilon_1 \epsilon_2}(t_2, t_1; c) = -iM\xi^{-1} [\epsilon_1 \ddot{g}_{-\epsilon_1}(t_1 + t_2) - \epsilon_1 \ddot{g}_{\epsilon_2 \epsilon_1}(t_2)] \\ + cM\xi^{-2} [\ddot{g}_{-\epsilon_1}(t_1 + t_2) + \ddot{g}_{\epsilon_2 \epsilon_1}(t_2)], \quad (24)$$

$$R_{\epsilon_1}^{(1)}(t_1; c) = \exp\{-i\epsilon_1 \omega_g t_1 - g_{-\epsilon_1}(t_1) - 2i\epsilon_1 c \xi^{-1} \dot{g}_{-\epsilon_1}(t_1) \\ + c^2 [\xi^{-2} \ddot{g}_{-\epsilon_1}(t_1) + \frac{1}{2} \ddot{g}(0)]\}. \quad (25)$$

Here $W_e = W_+$ and $W_g = W_-$. The Brownian oscillator model provides a picture in terms of wave packets in phase space that can be calculated semiclassically. Using a classical Langevin equation, Yan and Mukamel¹ derived closed expressions for the wave packets. The equations presented here generalize these results in two respects. (i) We use a microscopic description of the bath, which provides a consistent treatment of relaxation and dephasing

at all temperatures. The Langevin equation used previously is valid at high temperatures. Yan and Mukamel showed how the expression for the response function can be obtained from the Langevin equation by including the fluctuation dissipation theorem. However, the expression of the wave packets was given only in the high-temperature limit, since the semiclassical-Langevin-equation approach cannot keep track of the quantum coherence between the system and the noise source (the heat bath). This coherence is less important at high temperatures because of the fast dephasing but becomes dominant at low temperatures. (ii) We allow for an arbitrary dependence of the transition dipole moment on nuclear coordinates and thus relax the Condon approximation.

Using Eqs. (18)–(20) with Eqs. (9)–(13) and Eq. (21), we performed numerical calculations for the probe absorption spectrum and the wave packets for different temperatures $T = 100$ K and $T = 300$ K. Below we present the separate contributions from the particle and the hole in configuration space:

$$W_e(q; t) \equiv \int dp W_+^{(2)}(p, q; t), \quad W_g(q; t) \equiv \int dp W_-^{(2)}(p, q; t). \quad (26)$$

The calculations performed for the Condon case ($c = 0$) and the non-Condon case ($c = 0.1\sqrt{M\omega_0/\hbar}$) are denoted by (a) and (b), respectively, in Figs. 2–7 below. We assume that the damping induced by the heat bath is frequency independent, and it is denoted by γ (Ohmic dissipation). The phase function is then expressed as

$$g_{\pm}(t) = \lambda \left\{ \left[\frac{\lambda_1^2}{2\xi\omega_0^2} [\exp(-\lambda_2 t) + \lambda_2 t - 1] \coth\left(\frac{i\beta\hbar\lambda_2}{2}\right) \right. \right. \\ \left. \left. - \frac{\lambda_2^2}{2\xi\omega_0^2} [\exp(-\lambda_1 t) + \lambda_1 t - 1] \coth\left(\frac{i\beta\hbar\lambda_1}{2}\right) \right] \right. \\ \left. - \frac{4\gamma\omega_0^2}{\beta\hbar} \sum_{n=1}^{\infty} \frac{\exp(-\nu_n t) + \nu_n t - 1}{\nu_n [(\omega_0^2 + \nu_n^2)^2 - \gamma^2 \nu_n^2]} \right. \\ \left. \pm i\lambda \left\{ \exp(-\gamma t/2) \left[\frac{\gamma^2/2 - \omega_0^2}{\zeta\omega_0^2} \sin(\zeta t) + \frac{\gamma}{\omega_0^2} \cos(\zeta t) \right] \right. \right. \\ \left. \left. + t - \frac{\gamma}{\omega_0^2} \right\} \right\}, \quad (27)$$

where $\nu_n = 2\pi n/\hbar\beta$ and

$$\lambda_1 = \frac{\gamma}{2} + i\zeta, \quad \lambda_2 = \frac{\gamma}{2} - i\zeta, \quad \zeta = (\omega_0^2 - \gamma^2/4)^{1/2}. \quad (28)$$

This expression interpolates between several important limits:

Coherent motion limit ($\gamma \rightarrow 0$),

$$g_{\pm}(t) = \frac{\lambda}{\omega_0} [1 - \cos(\omega_0 t)] \coth\left(\frac{\beta\hbar\omega_0}{2}\right) \quad (29)$$

$$\pm \frac{i\lambda}{\omega_0} [\omega_0 t - \sin(\omega_0 t)]; \quad (29)$$

Strongly damped limit ($\gamma \gg \omega_0$ and $\Lambda \equiv \omega_0^2/\gamma$),

$$g_{\pm}(t) = \frac{2\lambda}{\beta\Lambda^2} [\exp(-\Lambda t) + \Lambda t - 1] \pm i \frac{\lambda}{\Lambda} [\exp(-\Lambda t) + \Lambda t - 1]. \quad (31)$$

$$g_{\pm}(t) = \frac{\lambda}{\Lambda} \left[(e^{-\Lambda t} + \Lambda t - 1) \cot(\hbar\beta\Lambda/2) + \frac{4\Lambda^2}{\beta\hbar} \sum_{n=1}^{\infty} \frac{e^{-\nu_n t} + \nu_n t - 1}{\nu_n(\nu_n^2 - \Lambda^2)} \right] \pm i \frac{\lambda}{\Lambda} (e^{-\Lambda t} + \Lambda t - 1); \quad (30)$$

Strongly damped at high temperature limit ($\gamma \gg \omega_0$, $\Lambda \equiv \omega_0^2/\gamma$, and $\beta\hbar\Lambda \ll 1$),

We first show the time evolution of the wave packets of the particle (Fig. 2) and the hole (Fig. 3) for an underdamped mode, $\gamma = 40 \text{ cm}^{-1}$ at $T = 100 \text{ K}$ and $T = 300 \text{ K}$. The frequency and the dimensionless displacement are given by $\omega_0 = 600 \text{ cm}^{-1}$ and $d \equiv D\sqrt{M\omega_0/\hbar} = 1.0$. As is seen from Fig. 2, the particle moves from the initial posi-

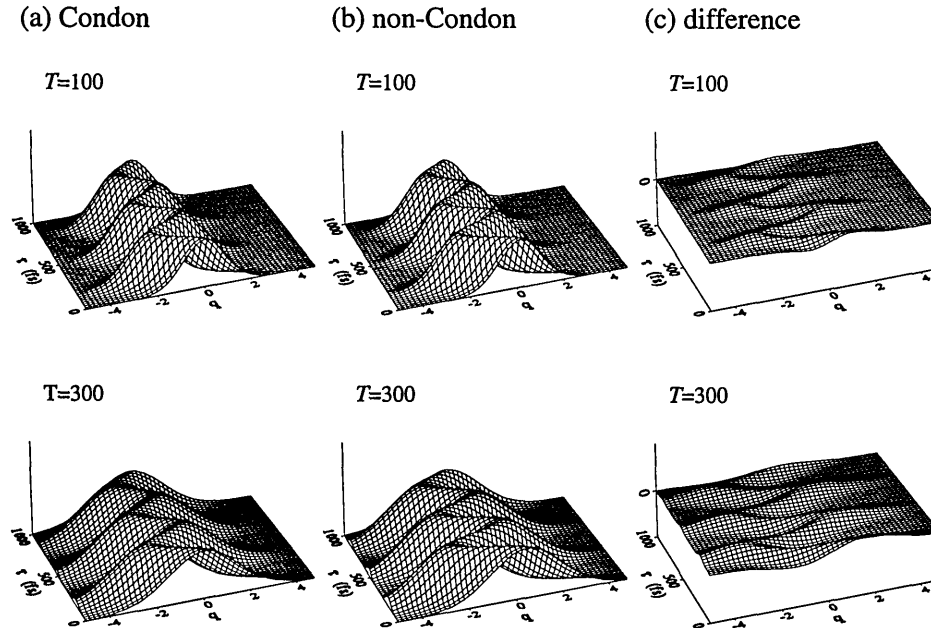


Fig. 2. Time evolution of the wave packet of the particle for the underdamped mode (the unit of q is $\sqrt{\hbar/M\omega_0}$) at $T = 100 \text{ K}$ and $T = 300 \text{ K}$ for (a) the Condon approximation, (b) the non-Condon interaction, and (c) their difference.

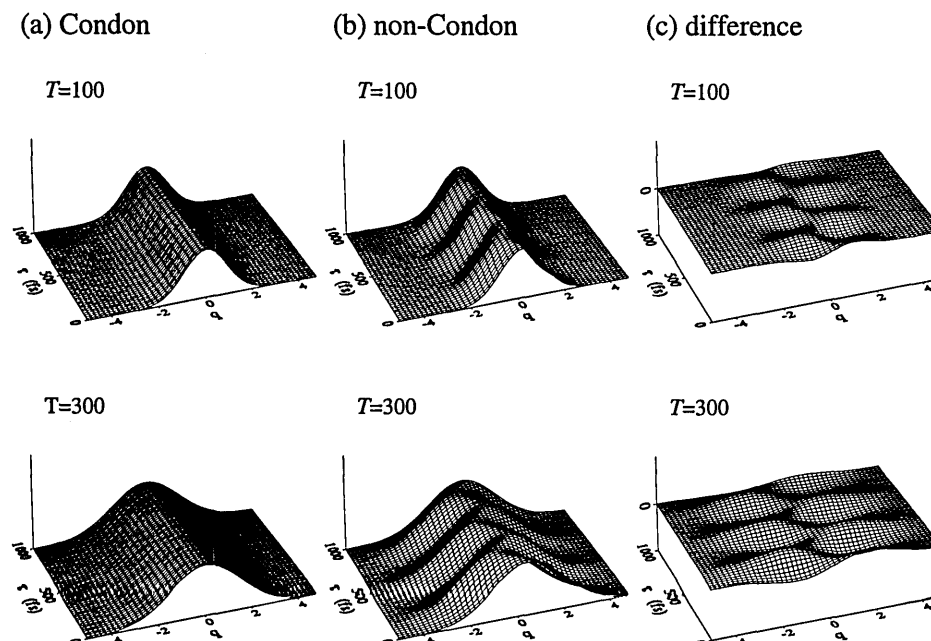


Fig. 3. Time evolution of the wave packet of the hole for the underdamped mode at $T = 100 \text{ K}$ and $T = 300 \text{ K}$ for (a) the Condon approximation, (b) the non-Condon interaction, and (c) their difference.

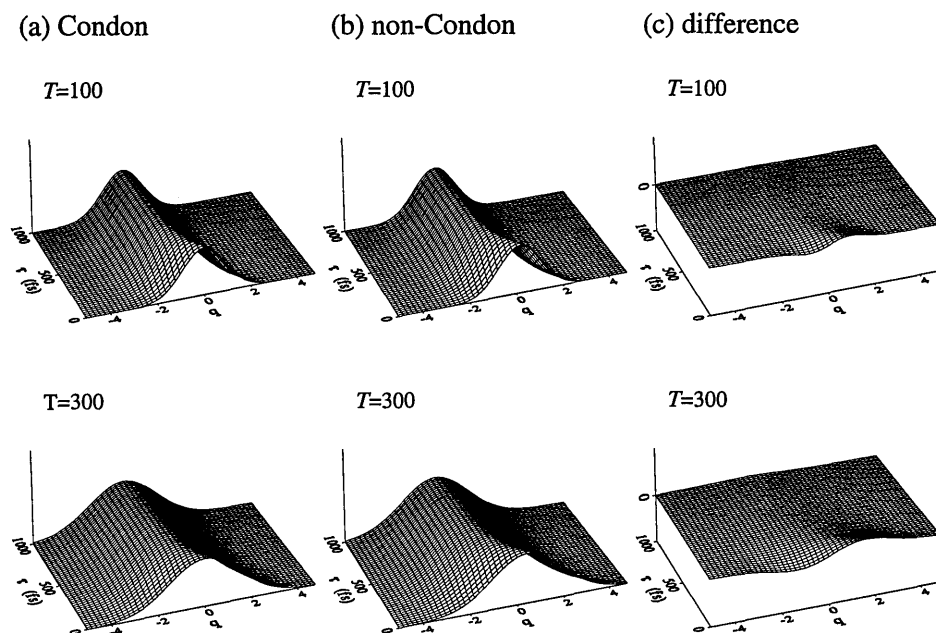


Fig. 4. Time evolution of the wave packet of the particle for the overdamped mode at $T = 100$ K and $T = 300$ K for (a) the Condon approximation, (b) the non-Condon interaction, and (c) their difference.

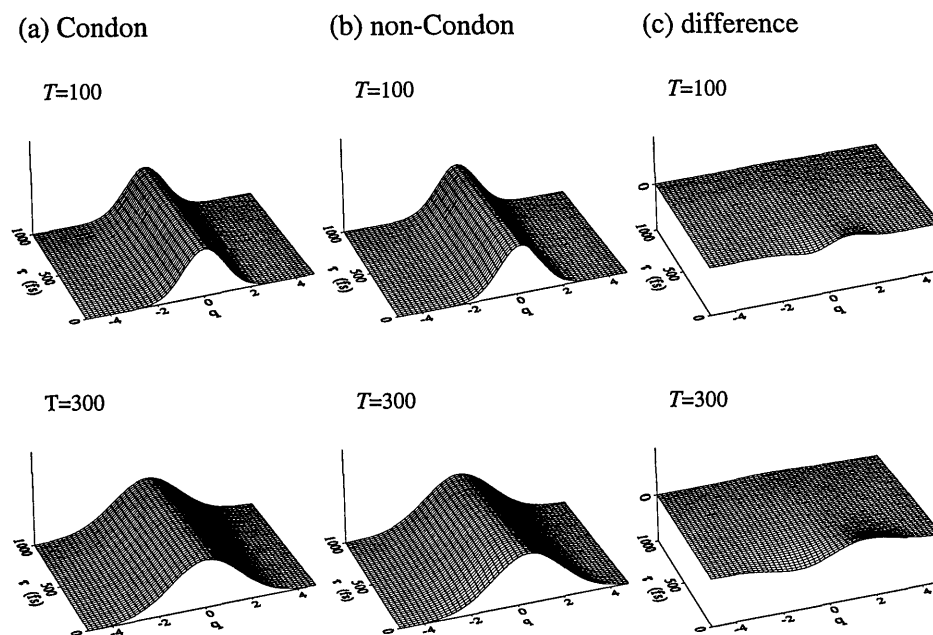


Fig. 5. Time evolution of the wave packet of the particle for the overdamped mode at $T = 100$ K and $T = 300$ K for (a) the Condon approximation, (b) the non-Condon interaction, and (c) their difference.

tion to the equilibrium state (the bottom of the excited-state potential) with a coherent oscillation, both for the Condon and the non-Condon cases. This is seen from Eq. (29). However, the hole in Fig. 3, which in the Condon case does not change its position and shape, slightly oscillates in the non-Condon case. Under the Condon approximation, the impulsive pump pulse creates a particle in the excited state without changing the Gaussian shape of the wave packet in the ground state. Then the shape of the hole wave packet is also Gaussian and cannot move in the harmonic potential. However, in the non-Condon case the coordinate-dependent dipole operator affects the shape of the ground equilibrium state.

Figures 4 and 5 show the time evolution of the wave packets of the particle (Fig. 4) and the hole (Fig. 5) for an overdamped mode $\gamma = 2000$ cm^{-1} , $\omega_0 = 600$ cm^{-1} , and $d = 1$ at $T = 100$ K and $T = 300$ K. As is seen from Fig. 4, the motion of the particle is critically damped in both the Condon and the non-Condon cases [see Eqs. (30) and (31)]. The hole motion is also strongly suppressed by the heat bath and, even with non-Condon interaction, the hole cannot move and shows behavior similar to the Condon case. The peak positions of the particle and the hole, however, shift to the positive side for the non-Condon case, because of the Condon dipole interaction Eq. (4). As is seen from the figures, this shift becomes large at $T =$

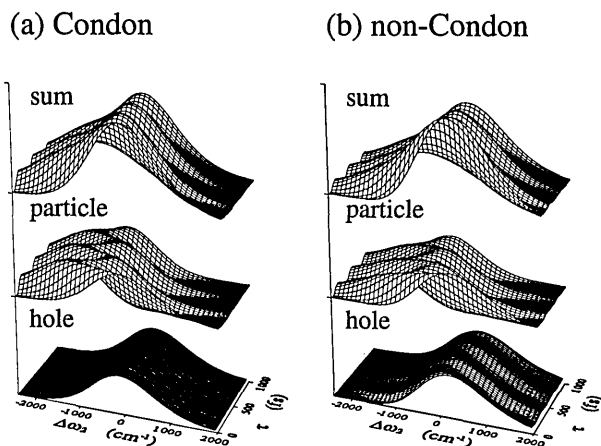


Fig. 6. Impulsive pump-probe spectrum for the two-mode case $\gamma = 40 \text{ cm}^{-1}$ and $\gamma = 2000 \text{ cm}^{-1}$ at the low temperature $T = 100 \text{ K}$. Here we define $\Delta\omega = \omega_2 - \Omega_2 - \omega_{eg}$. (a) is for the Condon approximation; (b) is for the non-Condon interaction. In each of these, we display the contributions of the hole, the particle, and their sum separately.

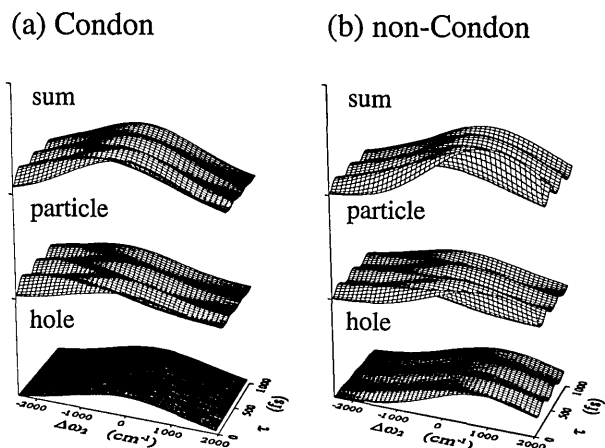


Fig. 7. Impulsive pump-probe spectrum for the two-modes case at the high temperature $T = 300 \text{ K}$. Other parameters are the same as in Fig. 6.

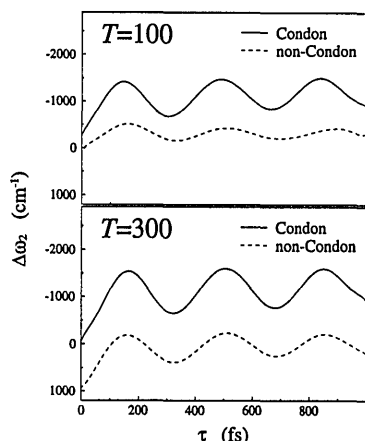


Fig. 8. Time evolution of the total absorption peaks in Figs. 6 ($T = 100$) and 7 ($T = 300$). Solid curves, the non-Condon approximation; dashed curves, the Condon approximation.

300 K. The reason for the large shifts at high temperatures in the case of the non-Condon interaction is as follows: before the pump excitation, the system is in the

ground equilibrium state and is localized if the temperature is low; however, it broadens if the temperature is high. As is seen from Eq. (4), the dipole element $\mu(q)$ is a linear function of q for small c . Since the population of particles at large q will increase at the higher temperatures, the non-Condon effect becomes larger.

We next calculated the absorption spectrum of a two-mode system that is described by the two nuclear coordinates q_1 and q_2 . For the two modes we took the underdamped mode discussed in Figs. 2 and 3 and the overdamped mode discussed in Figs. 4 and 5. We assume that the dipole moment has the form

$$\mu = \mu_0 \exp(c_1 q_1) \exp(c_2 q_2) \approx \mu_0 (1 + c_1 q_1 + c_2 q_2), \quad (32)$$

where c_1 and c_2 are the coupling constants, and we set $c_1 = c_2 = 0.1\sqrt{M\omega_0/\hbar}$. The corresponding response functions are given simply by the product of the single-mode response functions discussed above.

Figures 6 and 7 show the difference absorption spectrum for the different delay periods between the pump and the probe τ . Here we set $\Delta\omega \equiv \omega_2 - \Omega_2 - \omega_{eg}$. Figures 6(a) and 7(a) are for the Condon interaction, whereas 6(b) and 7(b) are for the non-Condon interaction. In each case we display the contributions of the hole, the particle, and their sum separately. The motion of the wave packets displayed in Figs. 2–5 is clearly reflected in the spectrum, and we can observe the motion of the hole and a temperature-dependent blue shift, which are both caused by the non-Condon interaction (see also Fig. 8).

ACKNOWLEDGMENTS

The support of the National Science Foundation and the U.S. Air Force Office of Scientific Research is gratefully acknowledged.

REFERENCES

1. Y. J. Yan and S. Mukamel, *J. Chem. Phys.* **88**, 5735 (1988); **89**, 5160 (1988).
2. S. Mukamel, *Adv. Chem. Phys.* **70**, 165 (1988); *Annu. Rev. Phys. Chem.* **41**, 647 (1990); L. E. Fried and S. Mukamel, *Adv. Chem. Phys.* **84**, 435 (1993).
3. M. Maroncelli, J. MacInnis, and G. R. Fleming, *Science* **234**, 1674 (1989).
4. P. F. Barbara and W. Jarzeba, *Adv. Photochem.* **15**, 1 (1990).
5. J. T. Fourkas and M. D. Fayer, *Acc. Chem. Res.* **25**, 227 (1992).
6. N. F. Scherer, R. J. Carlson, A. Matio, M. Du, A. J. Ruggiero, V. Romero-Rochin, J. A. Cina, G. R. Fleming, and S. A. Rice, *J. Chem. Phys.* **95**, 1487 (1991).
7. K. A. Nelson and E. P. Ippen, *Adv. Chem. Phys.* **75**, 1 (1989).
8. E. T. J. Nibbering, D. A. Wiersma, and K. Duppen, *Phys. Rev. Lett.* **66**, 2464 (1991).
9. P. C. Becker, H. L. Fragnito, J. Y. Bigot, C. H. Brito-Cruz, R. L. Fork, and C. V. Shank, *Phys. Rev. Lett.* **63**, 505 (1989); P. C. Becker, R. L. Fork, C. H. Brito-Cruz, J. P. Gordon, and C. V. Shank, *Phys. Rev. Lett.* **60**, 2462 (1988).
10. R. P. Feynman and F. L. Vernon, *Ann. Phys.* **24**, 118 (1963).
11. Y. Tanimura and S. Mukamel, *Phys. Rev. E* **47**, 118 (1993).
12. A. Garg, J. N. Onuchic, and V. Ambegaokar, *J. Chem. Phys.* **83**, 4491 (1985).
13. W. B. Bosma, Y. J. Yan, and S. Mukamel, *Phys. Rev. A* **42**, 6920 (1990).